INFECTION AND IMMUNITY, Mar. 2007, p. 1203–1213 Vol. 75, No. 3
0019-9567/07/$08.00+0 doi:10.1128/IAI.01702-06

Helicobacter pylori CagA Induces AGS Cell Elongation through a Cell Retraction Defect That Is Independent of Cdc42, Rac1, and Arp2/3▽†

Kevin M. Bourzac, Crystal M. Botham, and Karen Guillemin*

Institute of Molecular Biology, University of Oregon, Eugene, Oregon

Received 24 October 2006/Returned for modification 7 December 2006/Accepted 14 December 2006

***Helicobacter pylori*, which infects over one-half the world's population, is a significant risk factor in a spectrum of gastric diseases, including peptic ulcers and gastric cancer. Strains of *H. pylori* that deliver the effector molecule CagA into host cells via a type IV secretion system are associated with more severe disease outcomes. In a tissue culture model of infection, CagA delivery results in a dramatic cellular elongation referred to as the "hummingbird" phenotype, which is characterized by long, thin cellular extensions. These actin-based cytoskeletal rearrangements are reminiscent of structures that are regulated by Rho GTPases and the Arp2/3 complex. We tested whether these signaling pathways were important in the *H. pylori*-induced cell elongation phenotype. Contrary to our expectations, we found that these molecules are dispensable for cell elongation. Instead, time-lapse video microscopy revealed that cells infected by *cagA*$^+$ *H. pylori* become elongated because they fail to release their back ends during cell locomotion. Consistent with a model in which CagA causes cell elongation by inhibiting the disassembly of adhesive cell contacts at migrating cells' lagging ends, immunohistochemical analysis revealed that focal adhesion complexes persist at the distal tips of elongated cell projections. Thus, our data implicate a set of signaling molecules in the hummingbird phenotype that are different than the molecules previously suspected.**

Infections with strains of the gastric pathogen *Helicobacter pylori* that harbor the *cag* pathogenicity island (PAI) are associated with an increased risk for stomach ulcers and gastric cancer (6). The *cag* PAI is an approximately 40-kb cassette of genes that encode several homologues of a type IV secretion system (TFSS) and at least one delivered effector molecule, CagA. Once inside host cells, CagA localizes to the cell membrane, where it is recognized and phosphorylated by Src kinases (49, 50). Phosphorylated CagA binds to and activates the Src homology 2 (SH2) domain containing tyrosine phosphatase, SHP-2 (24). Inappropriate activation of SHP-2 and its downstream targets by CagA leads to abnormal cell signaling, which is likely to be the cause of many *cag* PAI-associated disease outcomes (for a review, see reference 7).

The *H. pylori*-host cell interaction is often modeled in vitro by coculture with a human gastric adenocarcinoma cell line, AGS. In AGS cells, CagA delivery and the subsequent altered cell signaling result in a dramatic actin-dependent cell morphological change known as the "hummingbird" phenotype, in which cells are transformed from a uniform polygonal shape into a severely elongated state characterized by the formation of needle-like projections (48). The hummingbird phenotype is strictly dependent on delivery of CagA into host cells and its subsequent tyrosine phosphorylation by host kinases, as demonstrated by the fact that cells infected with *H. pylori* lacking CagA, infected with *H. pylori* with a mutated CagA that cannot be phosphorylated, or treated with the Src kinase inhibitor PP2 do not elongate (3, 21, 48, 49). Additionally, this phenotype appears to be dependent on phosphorylated CagA's interaction with SHP-2 (22, 25). *H. pylori* infection also induces scattering in AGS cells, which is distinct from the hummingbird elongation phenotype in that it is at least partially CagA independent (1, 39). In MDCK cells, a polarized epithelial cell line, CagA-expressing cells lose their polarity, detach from their neighbors, and become motile with a phenotype reminiscent of an epithelial-to-mesenchymal transition, a process known to be important in metastasis (4). Therefore, understanding CagA's induction of cell morphological changes is critical for understanding CagA's link to cancer.

The needle-like projections which define the hummingbird phenotype are reminiscent of cellular structures such as neurite outgrowths and filapodium protrusions. Formation of these structures requires actin polymerization via the Arp2/3 complex and is often regulated by the Rho GTPases Cdc42 and Rac1. The Rho family GTPases Cdc42 and Rac1 are key mediators of actin dynamics that control cytoskeleton-based movement via signaling to the Arp2/3 complex through their downstream effectors N-WASP and WAVE, respectively (28, 44, 65, 66). Cdc42 and Rac1 signaling cascades are hijacked by several important human pathogens, both viral and bacterial, as part of their infectious life cycles (for reviews, see references 17 and 18). For example, the enteric pathogen *Salmonella enterica* serovar Typhimurium injects SopE and SopE2 effector proteins into host cells, which directly activate Cdc42 and Rac1 to induce membrane ruffling and bacterial uptake into nonphagocytic cells (9). Utilizing another mechanism, *Listeria monocytogenes* recruits Arp2/3 directly on the bacterial surface to initiate actin polymerization for intracellular motility and intercellular spread (63).

Previous studies have hinted that *H. pylori*'s effector protein CagA may induce the elongation phenotype through Cdc42 and Rac1 pathways as well. In one study, *H. pylori* infection was

* Corresponding author. Mailing address: Institute of Molecular Biology, University of Oregon, Eugene, OR 97403. Phone: (541) 346-5360. Fax: (541) 346-5891. E-mail: guillemin@molbio.uoregon.edu.

† Supplemental material for this article may be found at http://iai.asm.org/.

▽ Published ahead of print on 28 December 2006.

reported to stimulate Cdc42 and Rac1 activation and cause dramatic changes in the localization of these proteins, although these effects were dependent on an intact TFSS but independent of CagA delivery (11). In a DNA microarray study, we found that Cdc42 and its downstream effector, Cdc42 effector protein 2 (CEP2), were up-regulated in a CagA-specific manner (19). Additionally, the *H. pylori*-induced cell scattering phenotype appears to be dependent upon Rac1 signaling, although this study did not address cell elongation (53).

We hypothesized that the cytoskeletal rearrangements associated with the hummingbird cell elongation phenotype are Arp2/3-dependent, Cdc42- and Rac1-regulated events. However, our data refute this model and instead point to a new cellular mechanism of CagA-induced cell elongation which is likely to involve a set of molecular mechanisms different from the molecular mechanisms hypothesized previously.

MATERIALS AND METHODS

Bacterial strains and cell culture. Human gastric epithelial cells (AGS cells) were obtained from the American Type Culture Collection and were cultured in Dulbecco's modified Eagle's medium (DMEM) (Gibco) containing 10% fetal bovine serum (Gibco) and 10 μg/ml vancomycin. For infection experiments, cells were cultured in the same medium supplemented with 10% brucella broth (Difco). *H. pylori* wild-type strain G27 (12) and a *cagA* mutant (19) were maintained on blood agar plates containing Columbia agar (Difco) and 5% defibrillated horse blood (Hemostat) supplemented with 0.02 mg/ml β-cyclodextrin (Sigma), 8 mg/ml amphotericin B (Sigma), and 20 μg/ml vancomycin (Sigma) and incubated at 37°C in the presence of 10% CO_2. To prepare for infection experiments, bacteria were inoculated into infection media and grown overnight twice to an optical density at 600 nm of ~1.0 with agitation in anaerobe jars with Campygen packets (Oxoid) to supply a microaerophilic atmosphere. Just prior to infection, AGS cells were transferred to infection medium, *H. pylori* was added at a multiplicity of infection (MOI) of 100, the cultures were incubated for 15 min, and then nonadherent bacteria were removed with one change of medium. *S. enterica* serovar Typhimurium strain SL1344 expressing green fluorescent protein (GFP) (61) was a gift from Corrie Detweiler (University of Colorado, Boulder) and was grown in Luria broth (Difco). *L. monocytogenes* strain 10403S was a gift from Daniel Portnoy (University of California, Berkeley) and was grown in blood heart infusion medium (Difco).

Antibodies. For immunofluorescence experiments, cells were fixed for 10 min in 2% paraformaldehyde in 37.5 mM phosphate buffer with 750 mM lysine and 10 mM periodate and were permeabilized in blocking buffer (3% bovine serum albumin and 1% saponin in phosphate-buffered saline [PBS]) unless indicated otherwise. Chicken anti-GFP (Chemicon International) was used at a 1:2,500 dilution, and both mouse anti-*H. pylori* (MonoSan) and mouse anti-vinculin (Sigma) were used at a 1:200 dilution. Rabbit anti-Cdc42 (Santa Cruz) and mouse anti-Rac1 (Upsate) were used at a 1:100 dilution. To optimize visualization of Cdc42 localization, cells were first fixed in 4% paraformaldehyde–2% acetic acid for 2 min and then in 95% ethanol–5% acetic acid for 15 min, and then they were blocked in 8% bovine serum albumin in PBS before application of antibodies. Cy2 anti-chicken, Cy2 anti-mouse, Cy3 anti-rabbit (Jackson Immunologicals), Cy2 anti-rabbit, and Cy3 anti-mouse (Sigma) antibodies were used at a 1:200 dilution. Actin was visualized using tetramethyl rhodamine isocyanate, fluorescein isothiocyanate (Sigma), and Alexa Fluor 633-conjugated phalloidin (Molecular Probes) at dilutions of 1:500, 1:500, and 1:40, respectively.

For Western blotting, mouse anti-Rac1 (Upstate) was used at a 1:1,000 dilution, and mouse anti-Cdc42 (BD Transduction Labs) was diluted 1:250. Sheep anti-mouse and donkey anti-rabbit horseradish peroxidase-conjugated antibodies (Amersham Bioscience) were used at a 1:2,000 dilution.

DNA constructs. A plasmid for expression of the Cdc42/Rac interaction binding (CRIB) domain of p21-activated kinase fused to glutathione *S*-transferase (GST-CRIB) was kindly provided by Barbara Kazmierczak (originally from Richard Cerione, Cornell University, Ithaca, NY). Templates for Cdc42 and Rac1 N17 dominant negative mutants were kindly provided by Daniel Kalman (Emory University). WAVE1 template was provided by Shiro Suetsugu (University of Tokyo) and was used to create WAVE1ΔVPH (36). WAVE2ΔVPH (52) was created using cDNA from Open Biosystems (catalog no. MSH101-9204726), and N-WASP cDNA was obtained from the ATCC (catalog no. 10435323) and was used to create N-WASPΔVCA (amino acids 1 to 390) or the VCA domain alone (amino acids 391 to 507). These DNA constructs were cloned into pEGFP-C3 (Stratagene) for expression with N-terminal GFP fusions in mammalian cells. CEP2 was PCR amplified from AGS cell cDNA with a myc N-terminal tag and cloned into pcDNA3 (Invitrogen).

Cdc42/Rac1 activation assays. AGS cells were grown to confluence in 15-cm dishes. The medium was changed to infection medium, and cells were equilibrated for 3 h before addition of *H. pylori* at an MOI of 1:50. Cells were also infected with *S. enterica* serovar Typhimurium at an MOI of 1:50 in parallel experiments as a control. At different times, cells were washed once with ice-cold PBS and scraped into 750 μl of ice-cold lysis buffer (50 mM Tris-HCl [pH 7.5], 100 mM NaCl, 2 mM $MgCl_2$, 1 mM dithiothreitol, 1 mM *ortho*-vanadate, 10% glycerol, 1% NP-40, Complete protease inhibitor cocktail [Roche Bioscience]) containing 75 μl of GST-CRIB crude *Escherichia coli* lysate. Lysis was completed by four passages through a 23-gauge needle. Lysates were precleared by centrifugation at 4°C; then 50 μl was set aside for total Rho GTPase determination, and the remainder was incubated with glutathione agarose (Sigma) to capture GST-CRIB complexes. After three washes in excess lysis buffer, the protein was eluted from beads by boiling in 2× sodium dodecyl sulfate (SDS) sample buffer (125 mM Tris-HCl [pH 6.8], 20% glycerol, 2% SDS, 0.01% bromophenol blue), separated by SDS-polyacrylamide gel electrophoresis, and then transferred to a Hybond-P membrane (Amersham Bioscience) for Western blotting and detection via enhanced chemiluminescence with the ECL Plus detection reagent (Amersham Bioscience). Bands were visualized with a Storm 860 phosphorimaging system (Amersham Bioscience) and were quantified using the ImageQuant software (Molecular Dynamics).

Cell elongation assays. Cell elongation assays were performed as described previously (8). Briefly, AGS cells were seeded on glass coverslips and were transfected the next day using Lipofectamine 2000 (Invitrogen) according to the manufacturer's protocol. The transfection efficiency with AGS cells varied widely between 10% and 90% in a construct-dependent manner (unpublished observations). Cells were infected 24 h later at an MOI of 1:100, and the preparations were incubated for 6 h. In select experiments, cells were treated with 50 μM PP2 (Calbiochem) concurrent with addition of bacteria. Coverslips were very gently rinsed once with plain DMEM and then fixed and stained to visualize cells containing epitope-tagged proteins. Images of approximately 50 random fields of view at a magnification of ×200 were obtained using a Nikon TE2000 inverted microscope. The images were analyzed using Metamorph software to obtain length and breadth data for at least 200 transfected cells per condition.

Gentamicin protection assay. Gentamicin protection assays were performed essentially as described previously (2). AGS cells grown in six-well dishes were pretreated for 40 h with dimethyl sulfoxide (DMSO) alone or freshly reconstituted 10 μM GGTI-298 (Calbiochem). Confluent cells were then infected with *H. pylori*. Four hours after addition of bacteria, the medium was removed and replaced with normal infection medium (for counting total *H. pylori*) or infection medium supplemented with 200 μg/ml gentamicin (for counting internalized *H. pylori*). After an additional 4 h, cells were washed with two changes of medium to remove nonadherent extracellular bacteria and then scraped into and lysed in plain DMEM supplemented with 1% saponin before serial dilution and plating on blood agar for colony counting.

***L. monocytogenes* comet tail assay.** AGS cells were transfected 24 h before infection with GFP alone or GFP-VCA. *L. monocytogenes* was grown overnight at 30°C without shaking in blood heart infusion medium. Bacteria were then washed once in PBS and added to AGS cells at a dilution of 1:100 in DMEM containing 10% fetal bovine serum without antibiotics. One hour later, cells were washed three times with fresh medium to remove nonadherent bacteria. The cultures were incubated for another 30 min before gentamicin was added at a final concentration of 50 μg/ml. Internalized bacteria were then allowed to form comet tails for 5 h before fixation and processing for immunofluorescence analysis.

Time-lapse video microscopy. AGS cells were plated in four-well glass bottom Chamberwell slides (LabTek) and grown to 90% confluence. Immediately before the experiment, a pipette tip was used to scrape away cells and establish a central zone of sparse cells surrounded by a dense periphery, and then cells were infected as described above for cell elongation assays. PP2 was used at a concentration of 50 μM. A microaerophilic atmosphere was created in the wells by addition of an oxygen-sequestering enzyme (Oxyrase) at a 1:1,000 dilution before the chamber was sealed with a mineral oil overlay. Images were captured every 7 min for 9 h on a temperature-controlled stage adapted to the Nikon TE2000 inverted microscope.

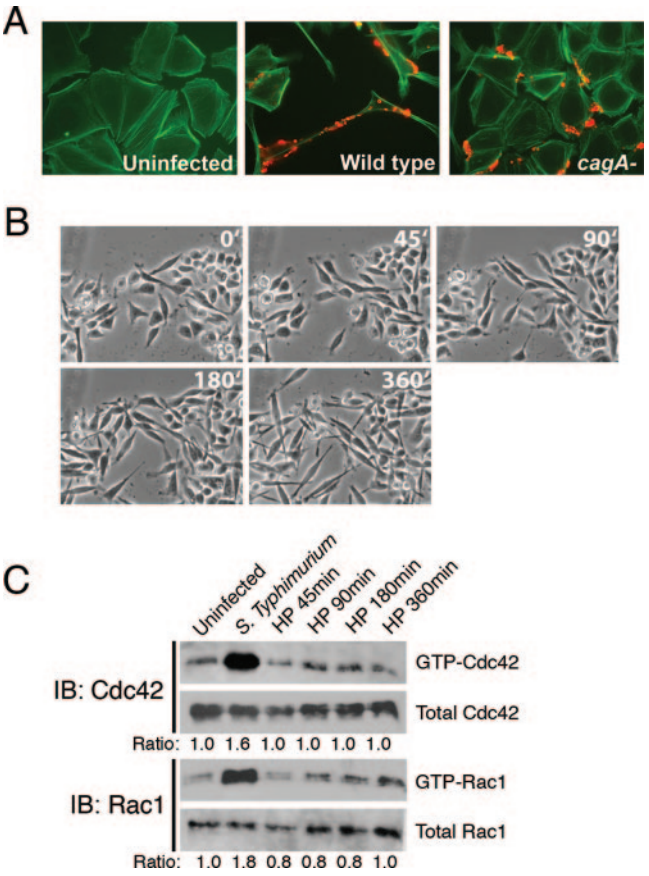

FIG. 1. Rho GTPases Cdc42 and Rac1 are not activated during an infection that leads to AGS cell elongation. (A) Uninfected AGS cells or AGS cells infected with wild-type *H. pylori* strain G27 or an isogenic *cagA* strain for 6 h were stained to reveal actin (green) and *H. pylori* (red). (B) *H. pylori*-infected AGS cells imaged with differential interference contrast optics for 6 h first exhibited the elongation phenotype within 3 h after addition of the bacteria. (C) Fractions of activated, GTP-bound Cdc42 and Rac1 were affinity purified and quantified in AGS cells that were mock infected (Uninfected), infected with *S. enterica* serovar Typhimurium for 45 min (*S. Typhimurium*), or infected with *H. pylori* (HP) for different times relative to the total pool of Cdc42 or Rac1. The ratios of the band intensity of activated GTPase to the band intensity of total GTPase, normalized to mock-infected controls, are indicated below the lanes. IB, immunoblot.

RESULTS

Rho GTPases Cdc42 and Rac1 are not activated or relocalized in response to *H. pylori* strain G27 infection. *H. pylori* infection of AGS cells results in an elongated cell morphology that has been termed the hummingbird phenotype and is "characterized by spreading and elongated growth of the cell, the presence of lamellipodia (thin actin sheets present at the edge of the cell), and filapodia (finger-like protrusions containing a tight bundle of actin filaments)" (48). Uninfected AGS cells are polygonal (Fig. 1A). The elongated phenotype induced by infection with wild-type *H. pylori* is dependent on CagA delivery since AGS cells infected with a *cagA H. pylori* mutant resemble uninfected cells (Fig. 1A).

Rho family GTPases play a central role in the formation of both lamellipodia and filapodia via their actions on the actin cytoskeleton (28, 44, 65, 66) and are a frequent target of bacterial pathogens (17). Churin et al. reported that the Rho family GTPases Cdc42 and Rac1 were activated in response to infection with *H. pylori* strain P1 in a manner dependent on the presence of a functional TFSS, although they did not find that activation required CagA (11). We wanted to know if the activity of Cdc42 and Rac1 increases following infection with wild-type *H. pylori* strain G27. Under our conditions, cell elongation was observed as soon as 3 h postinfection (Fig. 1B). To measure Cdc42 and Rac1 activation, we affinity precipitated activated Rho GTPases from cell lysates using glutathione *S*-transferase fused to the Cdc42/Rac1 interaction domain of p21-activated kinase (5). As a positive control for Cdc42 and Rac1 activation, cells were infected in parallel with *S. enterica* serovar Typhimurium strain SL1344, which activates both Cdc42 and Rac1 via delivery of the effector proteins SopE and SopE2 (13). We detected basal Cdc42 and Rac1 activity in control cells, and this activity was greatly increased during *S. enterica* serovar Typhimurium infection. However, we did not detect any increased activation of Cdc42 or Rac1 during an *H. pylori* infection, even at times when cells were visibly elongated (Fig. 1C).

Churin et al. also reported that Cdc42 and Rac1 proteins relocalize to the points of bacterial attachment on AGS cells infected with *cagA H. pylori* mutants but not on AGS cells infected with TFSS *H. pylori* mutants derived from strain P1 (11). We tested whether we could observe the relocalization of Cdc42 and Rac1 under our infection conditions with strain G27 that resulted in cell elongation.

AGS cells were infected with *H. pylori* for 3 or 6 h and stained to reveal bacteria and Cdc42 or Rac1. Uninfected cells and cells infected with *S. enterica* serovar Typhimurium SL1344 for 45 min as controls represented basal and activated conditions, respectively. We chose *S. enterica* serovar Typhimurium infection as a positive control because we observed robust Cdc42 and Rac1 activation under these conditions (Fig. 1C) and because *S. enterica* serovar Typhimurium infection of polarized MDCK cells reportedly causes apical accumulation of these proteins (55). To ensure that the staining patterns that we observed were not due to nonspecific binding by the secondary antibodies, we performed control experiments in which the primary antibodies were omitted, which eliminated all staining of any cellular structures (data not shown). In our experiments, the localization of both Cdc42 and Rac1 remained unchanged under all conditions, even when cells were infected with *S. enterica* serovar Typhimurium. Cdc42 was always observed surrounding the nuclear envelope in the region of the endoplasmic reticulum and Golgi apparatus (Fig. 2A to D). This localization pattern is in accordance with observations described by other workers for nonpolarized cells (16, 35). Perinuclear localization was also observed for Rac1 in addition to staining along the lamellipodia (Fig. 2E to H), which is also consistent with previous observations (15). Although cells were covered with attached *H. pylori* by 6 h postinfection (Fig. 2C, D, G, and H), there was no distinct pattern of bacterial colocalization with either Cdc42 or Rac1.

Cdc42 and Rac1 are not required for elongation. Next, we asked if Cdc42 or Rac1 was necessary for *H. pylori*-induced elongation by comparing the shape of *H. pylori*-infected cells that were transfected with GFP-tagged dominant negative (N17) alleles of Cdc42 and Rac1 to the shape of transfected

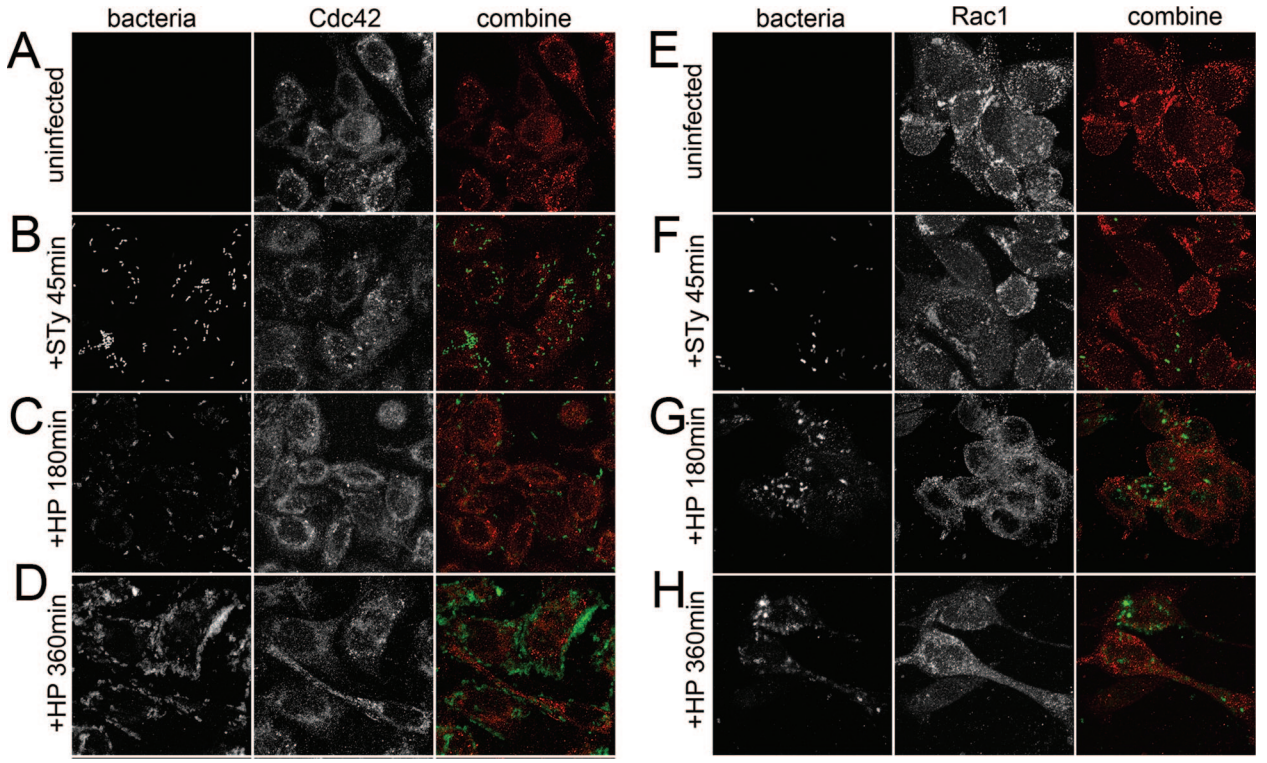

FIG. 2. Localizations of both Cdc42 and Rac1 remain unchanged during infection with *H. pylori* or *S. enterica* serovar Typhimurium. Mock-infected cells (uninfected) (A and E), cells infected with *S. enterica* serovar Typhimurium for 45 min (+Sty 45 min) (B and F), or cells infected with *H. pylori* for 3 h (+HP 180 min) (C and G) or 6 h (+HP 360 min) (D and H) were stained to reveal total Cdc42 (A to D) or Rac1 (E to H). Cdc42 and Rac1 are red, while bacteria are green.

but uninfected cells. Comparisons of reports of CagA-induced cell elongation have been complicated by the use of multiple different definitions of *H. pylori*-induced cell morphology changes. Here, we used a quantitative measurement of *H. pylori*-induced cell elongation (8). Measurement of individual elongated cells in a population is extremely difficult due to overlapping cells (Fig. 1B, lower right panel). Therefore, we transfected cells with GFP or GFP fusion proteins, which allowed these cells to be easily distinguished from their nontransfected neighbors. We then used the Metamorph imaging software to determine the lengths (the longest distance across a cell) and breadths (the longest distance perpendicular to the length) of 200 to 400 transfected cells from at least 50 random fields of view in each experiment (Fig. 3A). For each transfected construct, we then compared the length-to-breadth (L/B) ratios of cells infected with *H. pylori* for 6 h with the L/B ratios of their transfected but uninfected counterparts.

Using the L/B ratio, we were able to document the consistent cell elongation response of AGS cells to *H. pylori* infection. We observed some variation between experiments in the extent of cell elongation, but the *H. pylori*-infected cells always differed significantly from the uninfected controls ($P < 1 \times 10^{-3}$). Therefore, data from individual experiments are shown here, but they are representative of a minimum of three independent trials. In a representative experiment, GFP-transfected AGS cells that were infected with *H. pylori* showed an average 1.3-fold increase in the L/B ratio compared to uninfected cells that were transfected in parallel (Fig. 3B). Cell elongation has been shown to require CagA phosphorylation by Src family member kinases, which are inhibited by treatment with the tyrosine kinase inhibitor PP2 (3, 49). The L/B ratios of infected cells that were concurrently treated with 50 μM PP2 were not statistically different than the L/B ratios of uninfected cells ($P > 0.05$) (Fig. 3B).

Next, we tested whether dominant negative alleles of Cdc42 and Rac1 could block *H. pylori*-induced cell elongation. The average L/B ratio for cells expressing GFP-Cdc42(N17) or GFP-Rac1(N17) and infected with *H. pylori* was found to be 1.3-fold greater than the average L/B ratio for uninfected controls, similar to the results obtained for GFP-transfected cells (Fig. 3C and D). Identical results were obtained using myc rather than GFP-tagged alleles that were expressed from a different mammalian expression vector (not shown). We concluded that Cdc42 or Rac1 inhibition alone is not sufficient to block the hummingbird phenotype.

Cdc42 and Rac1 can function redundantly, as demonstrated by the observation that inhibition of Cdc42 or Rac1 alone attenuates but does not completely inhibit *S. enterica* serovar Typhimurium invasion (59). In our transfection assays we were limited to inhibition of only one pathway at a time and could not exclude the possibility that CagA-induced elongation, like *S. enterica* serovar Typhimurium invasion, occurs through either Cdc42 or Rac1 pathways. Therefore, we wanted to test conditions in which both Cdc42 and Rac1 were simultaneously inhibited. Rho family GTPases, including Cdc42 and Rac1, undergo prenylation with a geranylgeranyl moiety through the

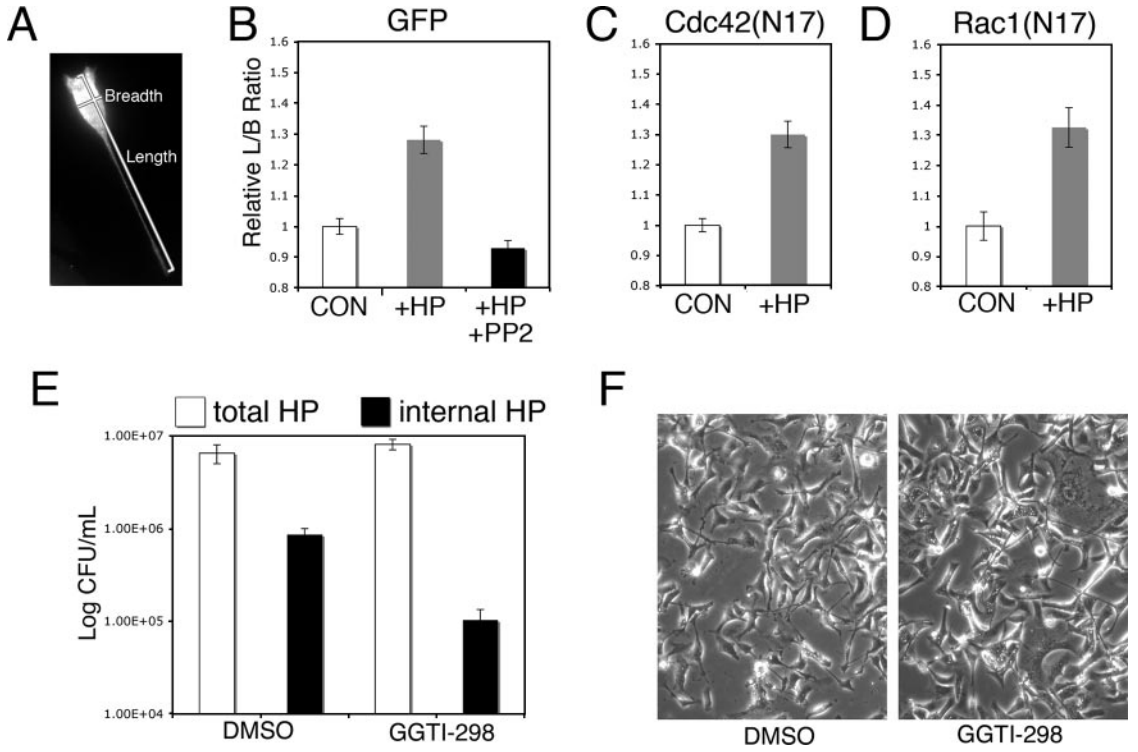

FIG. 3. Cell elongation is independent of Cdc42 and Rac1. (A) Cell elongation was quantified by determining the ratio of cell length to cell breadth, as indicated. (B to D) Cell elongation measurements for AGS cells transfected with GFP alone (B) or with dominant negative alleles of GFP-Cdc42 (C) or GFP-Rac1 (D). In all cases the *H. pylori* (HP)-infected cells were significantly elongated compared with the uninfected cells ($P < 10^{-3}$), whereas cells treated with 50 μM PP2 inhibitor in the presence of *H. pylori* (B) did not differ from uninfected cells ($P > 0.05$). (E) *H. pylori* internalization in AGS cells mock treated with DMSO or with GGTI-298 for 40 h prior to *H. pylori* infection. (F) Cell elongation occurred in both AGS cells mock treated with DMSO and AGS cells treated with GGTI-298 for 40 h, followed by 6 h of infection with *H. pylori*. CON, control. The error bars indicate standard errors.

activity of geranylgeranyl transferase. This modification is required for Rho GTPase localization to the plasma membrane and participation in normal signaling (65). GGTI-298 is a specific and selective inhibitor of geranylgeranyl transferase at a concentration of 10 μM (62). Therefore, we used GGTI-298 to inhibit Rho GTPases in AGS cells and assayed aspects of the AGS response to *H. pylori* infection.

Although *H. pylori* remains predominantly extracellular during coculture with tissue culture cells, a small *H. pylori* population is internalized. This phenotype is independent of the *cag* PAI but dependent on host cell actin networks (2, 30, 41). We found that the ability of GGTI-298-treated AGS cells to internalize *H. pylori* was reduced by nearly an order of magnitude (Fig. 3E). Thus, our results indicated that the GGTI-298 inhibitor was effective at blocking at least one host cell activity thought to be dependent on actin cytoskeleton dynamics.

Next, we tested whether GGTI-298 treatment of AGS cells blocked *H. pylori*-induced cell elongation. GGTI-298-treated cells were much more susceptible to *H. pylori*-induced cell death and were also resistant to transfection and thus not amenable to analysis using our length-to-breadth ratio assay (data not shown). However, as determined by differential interference contrast microscopy, we observed no difference in elongation in response to *H. pylori* infection between GGTI-298-treated cells and cells treated with DMSO alone (Fig. 3F). Based on these findings together with our data obtained from infection of cells expressing dominant negative Rho GTPases, we concluded that cell elongation is independent of the activity of Cdc42 and Rac1.

Effector proteins downstream of Cdc42 and Rac1 are not required for elongation. Although our experiments did not uncover any role for Cdc42 and Rac1 in *H. pylori*-induced cell elongation, we wondered if CagA could directly manipulate the downstream effectors of these small Rho GTPases. During normal signaling, activated GTP-bound Cdc42 and Rac1 bind to their effectors N-WASP and WAVE, respectively. These proteins contain C-terminal veprin and cofilin homology regions and acidic domains (termed VCA in N-WASP and VPH in WAVE), which mediate interactions with actin and the Arp2/3 complex (37). In this way, both Cdc42 and Rac1 signal through parallel pathways to initiate actin polymerization via Arp2/3. C-terminal truncations of these proteins lacking the VCA or VPH domain are unable to bind Arp2/3 and act in a dominant negative manner (36, 40). Therefore, we transfected cells with a ΔVCA mutant of N-WASP and two WAVE isoforms (WAVE1ΔVPH and WAVE2ΔVPH) in our transfection and elongation assay. Again, we found that the dominant negative constructs had no effect on *H. pylori*-induced cell elongation (data not shown).

We also tested another downstream effector of Cdc42, CEP2, which we identified as a molecule that was strongly up-regulated in AGS cells in response to CagA delivery (19).

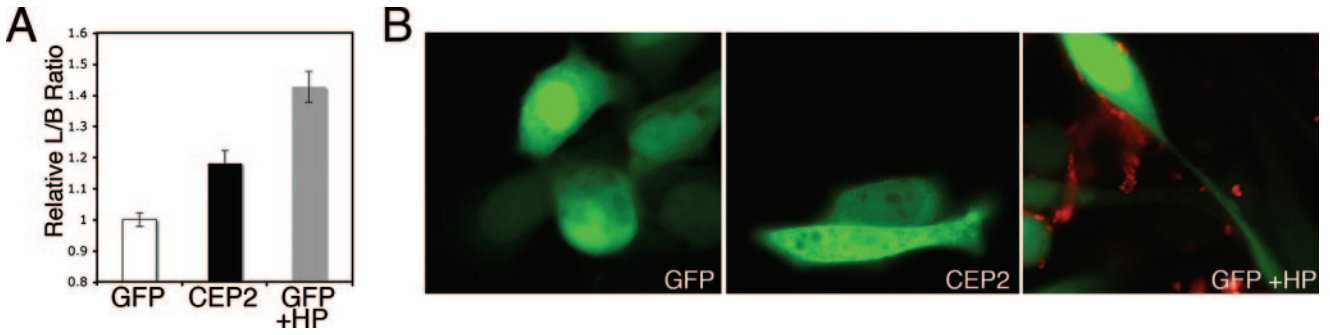

FIG. 4. Overexpression of CEP2 does not resemble *H. pylori* infection. Expression of the Cdc42 effector molecule CEP2 caused elongation of AGS cells (A), but the morphology of these cells did not resemble *H. pylori*-induced cell elongation (B). GFP or CEP2 is green, and *H. pylori* is red. HP, *H. pylori*. The error bars indicate standard errors.

Overexpression of CEP2 was reported to cause cell elongation in NIH-3T3 cells, and this activity was dependent on CEP2's ability to bind Cdc42 through its CRIB domain (26). We tested whether CEP2 expression in AGS cells could phenocopy CagA-induced cell elongation. Uninfected cells overexpressing CEP2 were compared to cells expressing GFP and cells expressing GFP that were infected with *H. pylori*. We found that CEP2 caused a modest but statistically significant increase in the average L/B ratio (Fig. 4A). However, CEP2-induced elongation did not phenocopy *H. pylori* infection either in magnitude (Fig. 4A) or in cell morphology (Fig. 4B). CEP2-transfected cells were indeed longer than GFP-transfected cells, but they lacked the extremely long needle-like projections observed in *H. pylori*-infected cells (Fig. 4B). We concluded that CEP2 signaling is not sufficient to cause the same elongation phenotype as the phenotype induced by *H. pylori*.

CagA-induced cell elongation is Arp2/3 independent. Cdc42 and Rac1 exert their effects on the actin cytoskeleton by activation of the Arp2/3 complex, which is the target of the Cdc42 and Rac1 effectors N-WASP and WAVE. However, Arp2/3 can be activated by several other inputs as well (64). Therefore, we tested whether the Arp2/3 complex itself was required for cell elongation by determining the L/B ratios of cells transfected with the dominant negative VCA domain of N-WASP. This construct inappropriately activates Arp2/3 and displaces it from normal regulation, effectively suppressing its activity (20, 31, 32, 40).

The bacterial pathogen *L. monocytogenes* polymerizes actin on its surface, enabling it to move within host cells and facilitate intracellular spread via activation of the Arp2/3 complex (63). The resulting actin comet tails can be blocked by inhibition of Arp2/3 via overexpression of VCA (34). We transfected cells with GFP alone or GFP fused to the VCA domain of N-WASP (GFP-VCA) and then infected the cells with *L. monocytogenes* 1043S. We observed comet tails in about 15% of the AGS cells transfected with GFP. However, the level of comet tail formation was 5% in cells expressing GFP-VCA (Fig. 5A and B). This level of comet tail formation inhibition is similar to the level seen when RNA interference silencing of the Arp2 complex was used, which is another effective method of blocking Arp2/3 function (14), and demonstrated that the N-WASP VCA domain significantly reduced Arp2/3 activity in AGS cells. We then tested whether inhibition of Arp2/3 in AGS cells blocked *H. pylori*-induced cell elongation. We found that the average L/B ratio of AGS cells expressing the GFP-VCA construct increased approximately 1.3-fold in the presence of *H. pylori* (Fig. 5C), which was similar to the effect on

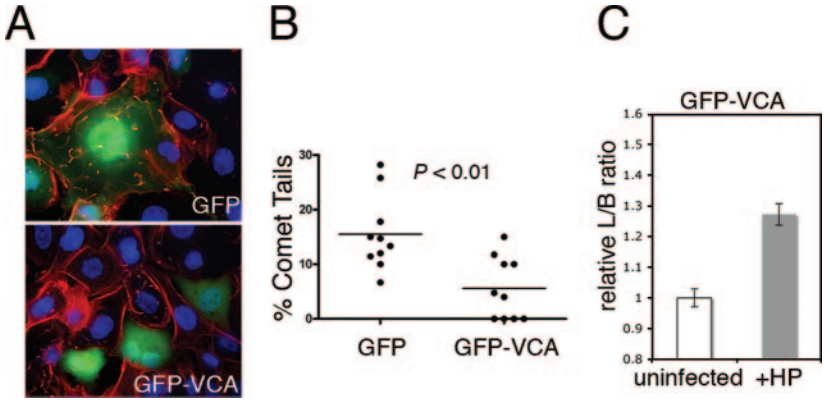

FIG. 5. *H. pylori*-induced elongation phenotype is Arp2/3 independent. (A) Actin-based comet tails were visualized in *L. monocytogenes*-infected AGS cells transfected with GFP or GFP-VCA (actin, red; transfected cells, green; cell and bacterial nuclei, blue). (B) Percentage of transfected cells with comet tails, quantified using 10 random fields of view. (C) Cells transfected with GFP-VCA elongated upon *H. pylori* infection. HP, *H. pylori*. The error bars indicate standard errors.

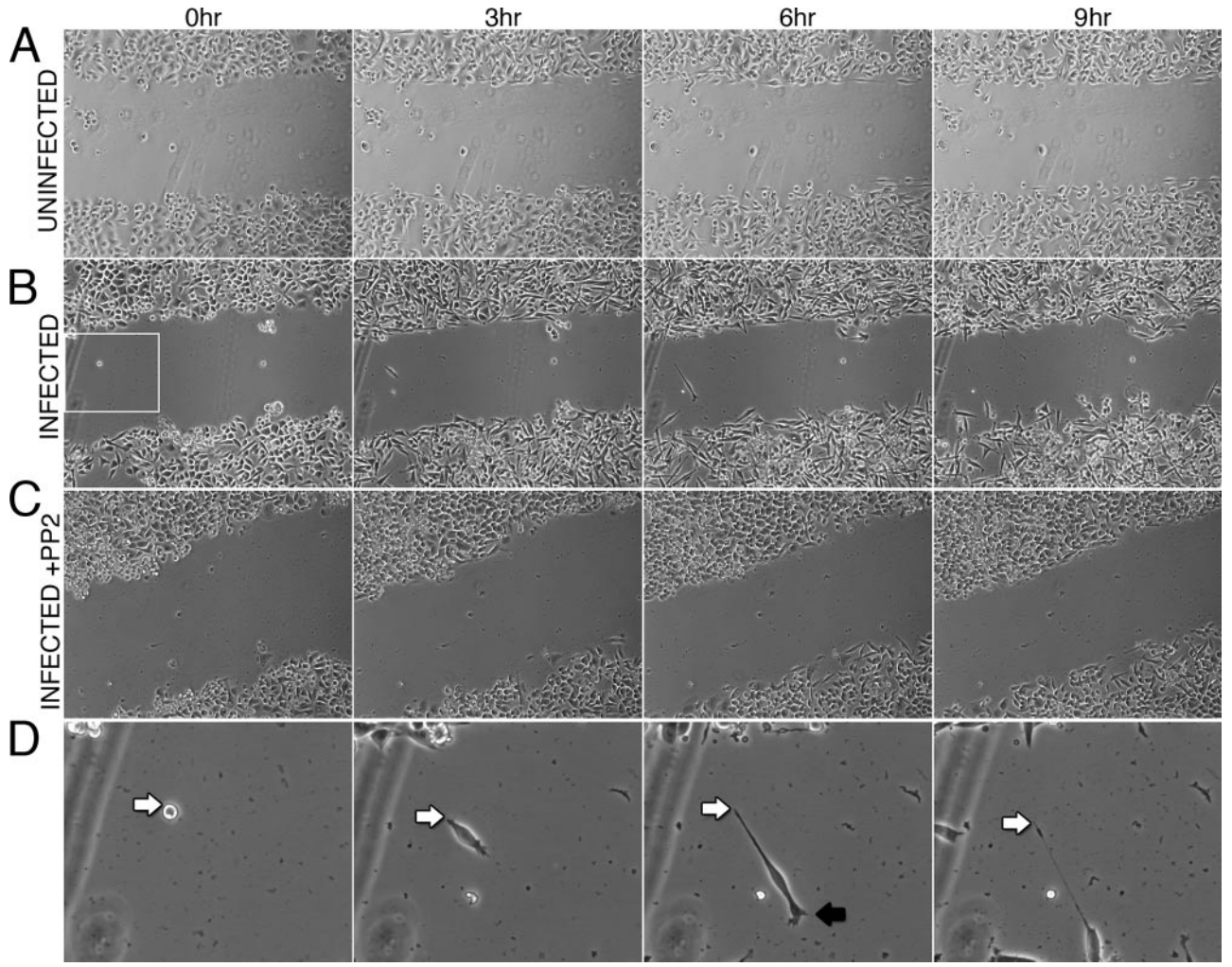

FIG. 6. *H. pylori*-infected cells exhibit retraction defects. (A to C) Still images from video time-lapse microscopy of uninfected cells (A), cells infected with *H. pylori* (B), and cells treated with 50 μM PP2 and infected with *H. pylori* (C). (D) Enlargement of the elongating cell enclosed in a box in panel B. The back and front ends of the cell are indicated by white and black arrows, respectively. Panels A to C were taken from time-lapse videos which are available in the supplemental material.

cells transfected with GFP alone (Fig. 3B and 4D). Therefore, we concluded that *H. pylori*-induced cell elongation is Arp2/3 independent.

Hummingbird phenotype results from a cell retraction defect. In order to better understand the hummingbird elongation phenotype, we used video time-lapse microscopy to observe *H. pylori*-infected AGS cells in real time. As expected, our videos showed that AGS cells infected with *H. pylori* undergo dramatic cellular elongation that becomes apparent within 3 h of infection, and this elongation is inhibited by PP2, a specific inhibitor of Src family kinases (Fig. 6A to C) (see movies in the supplemental material). To better understand AGS cell motility, we tracked the movement of individual cells for up to 9 h. We found that both infected and uninfected cells were quite motile and moved about stochastically, often changing direction. By tracking the cell nucleus with the ImageJ software, we plotted the movements of more than 25 individual cells chosen randomly from three fields of view for both uninfected and infected cells (Fig. 7A and B). The total distances traveled by cells under both conditions were not significantly different in the presence and in the absence of the bacteria, nor were the distances traveled from the point of origin significantly different (Fig. 7C and D).

When we examined more closely the movement of uninfected AGS cells, we observed that in general, cells moved forward by extension of a lamellipodium or pseudopodium which proceeded through many frames and was accompanied by intermittent and rapid retraction of the back end or uropod of the cell (see Movie 1 in the supplemental material). In some cases, a cell sent out multiple pseudopodia before choosing a direction of travel. Infected cells sent out protrusions with similar dynamics. However, as infected cells began to move, they failed to retract their rear ends and instead remained firmly attached, as shown in Fig. 6B and D. The result of such a retraction failure was that the cells became highly elongated due to the two opposing forces pulling on either end of the cell (see Movie 2 in the supplemental material). Often the taut, extended cells were observed to simply break apart under the

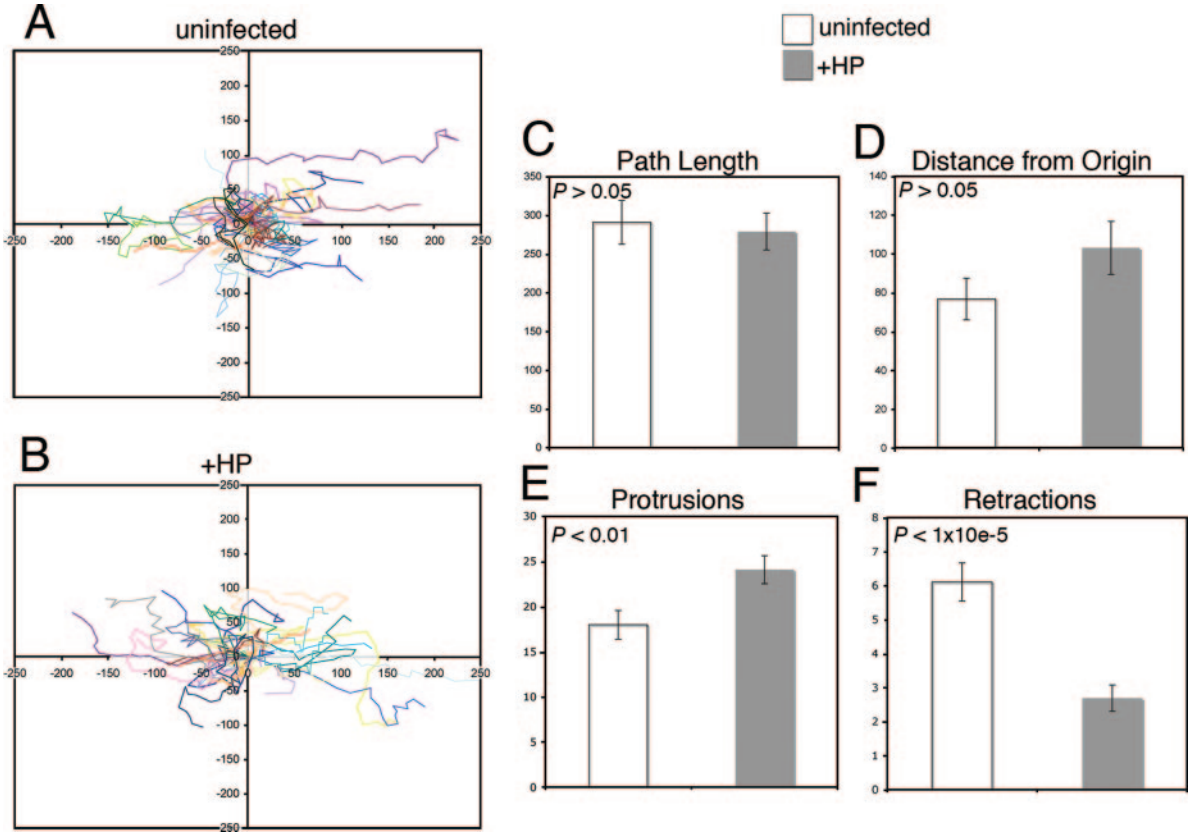

FIG. 7. *H. pylori*-infected cells undergo fewer cell retraction events. (A and B) Plots showing the movements of individual AGS cells over a 9-h time course for 28 uninfected cells (A) and 26 cells infected with *H. pylori* (HP) (B). (C to F) Average total path length traveled (C), average distance traveled from origin of the cell nuclei (D), and average numbers of cell protrusion (E) and retraction (F) events for both infected and uninfected cells. The *P* values for comparisons of the averages for uninfected and infected cells are indicated. The error bars indicate standard errors.

tension, leaving bits of cellular debris where their back ends had failed to retract.

To quantify this phenomenon, we monitored the protrusive and retractile behavior of the 54 individual cells analyzed in Fig. 7A to D. We first counted the number of frames during which a cell exhibited protrusive morphology, defined as an increase in cell surface area in the direction of cell movement between frames. Cells infected with *H. pylori* underwent slightly more protrusion events than uninfected cells underwent (Fig. 7E). We next counted retraction events in the same cells (a retraction event was defined as a decrease in the cell surface area between frames in the direction of cell movement) and found that infected AGS cells underwent far fewer retraction events than control cells underwent (Fig. 7F). Thus, we concluded that the hummingbird elongation phenotype is a result of a cell retraction defect.

Focal adhesions (FA) are large, multiprotein complexes that mediate interactions between cells and the substrate to which they adhere. Disassembly of FA at the cell's distal end is a crucial step in cell translocation (45). If our hypothesis that the hummingbird phenotype results from a retraction defect is correct, then we should observe focal adhesions inappropriately stabilized in the distal tips of cell protrusions. We examined the distribution of the FA in AGS cells by staining cells with an antibody to the FA component vinculin. We asked whether the locations of FA were different in infected and uninfected cells. Uninfected cells generally were polygonal and were decorated with FA complexes on the peripheral, basal surface (Fig. 8A). In contrast, the projections of infected cells showed no FA complexes along the length. Significantly, we observed FA complexes at the distal tips of cell projections. Based on our live imaging analysis showing that these cell projections are formed from the back ends of migrating cells, we interpreted the vinculin distribution as validation of our model that the hummingbird phenotype arises from a failure to disassemble FA at the cell uropod during cell migration (Fig. 8B and C).

DISCUSSION

Here we present the results of a detailed investigation of the hummingbird cell elongation phenotype in AGS cells following infection with *H. pylori*. Our real-time analysis of the elongation phenomenon revealed that this phenotype is due to a cell retraction defect rather than from filapodial protrusions. We found that AGS cells were intrinsically motile, and this motility was only moderately increased by infection with *H. pylori*. However, infection and subsequent CagA delivery resulted in a reduction in the number of cell retraction events. This observation is consistent with our finding that cell elongation is

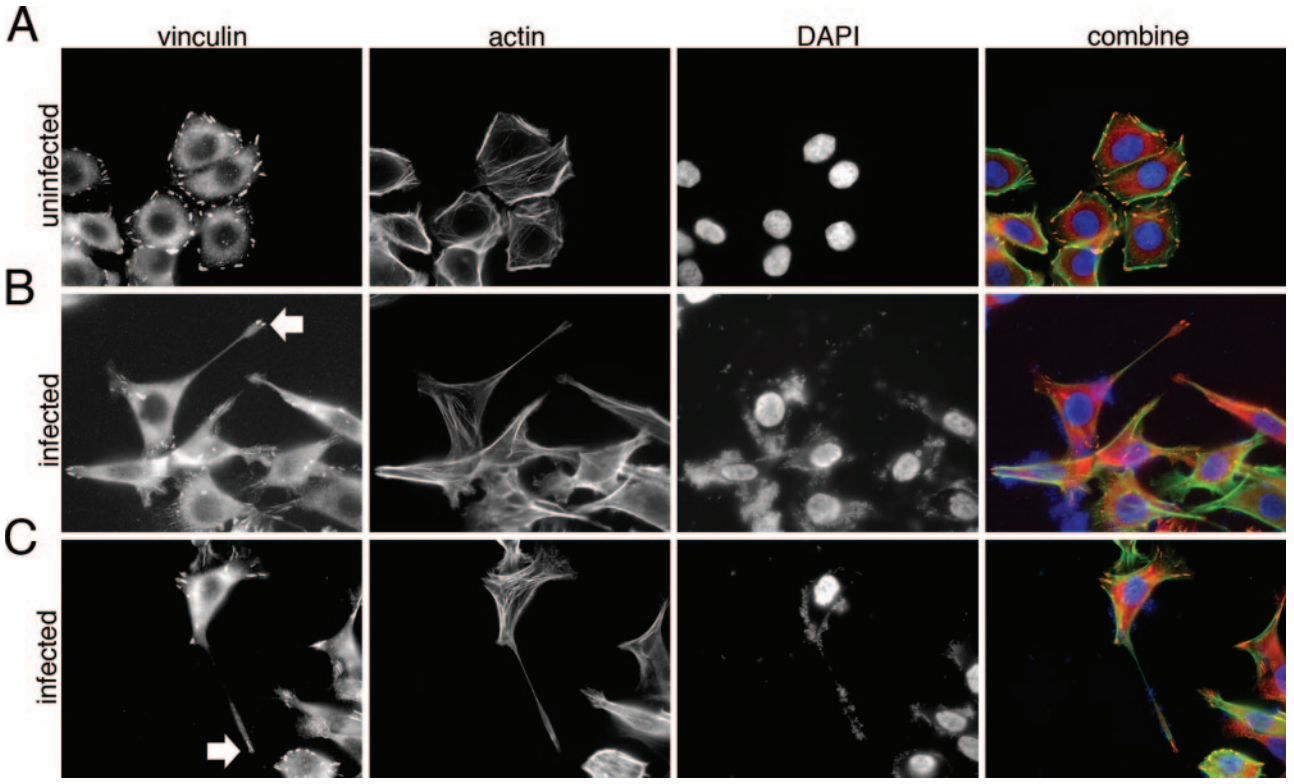

FIG. 8. *H. pylori*-infected cells maintain focal adhesion complexes at their distal tips. FA complexes in uninfected AGS cells (A) and cells infected for 6 h with *H. pylori* (B and C) were visualized with a vinculin antibody (red). The actin cytoskeleton (green) and host and bacterial cell nuclei (blue) were also stained. FA were located at the distal dips of elongated *H. pylori*-infected cells (arrows). DAPI, 4′,6′-diamidino-2-phenylindole.

independent of signaling pathways that regulate Arp2/3-dependent cell protrusion events.

As a first test of Rho GTPase signaling during *H. pylori* infection, we looked for changes in the activity or localization of these proteins during an elongation time course. We were able to detect Cdc42 and Rac1 activation in AGS cells infected with *S. enterica* serovar Typhimurium, but this assay could not detect similar activation in an *H. pylori* infection, nor did we observe relocalization of Cdc42 and Rac1 under conditions in which they were activated (when cells were infected with *S. enterica* serovar Typhimurium). Our analysis of Rho GTPase cellular distribution is consistent with other reports of nonpolarized cells indicating that total Rho GTPase localization does not correlate with GTP- or GDP-bound status and does not shift under GTPase-stimulating conditions (43). Subtle relocalization of a small subset of GFP-Rho GTPase fusion proteins in response to known stimulatory signals has been detected by high-resolution methods (15). In other studies workers have utilized fluorescence resonance energy transfer to track the fleeting changes in activated subsets of the GTPase pool with GFP-fused effectors (27, 29, 43). We attempted to use *S. enterica* serovar Typhimurium as a positive control for Cdc42 and Rac1 localization based on a previous report with MDCK cells that infection with this bacterium results in apical accumulation of these proteins (55). We observed no such localization change in our AGS cells, but AGS cells are nonpolarized and thus physiologically very different from MDCK cells. It is not clear why there is a discrepancy between our results and the results of Churin et al., who reported *cag* PAI-dependent but CagA (and thus elongation)-independent activation and change in localization of these proteins (11). It is possible that due to heterogeneity among *H. pylori* isolates, the strain that we tested (G27) lacks an as-yet-unidentified effector molecule responsible for Rho GTPase activation and localization. Such a putative effector, however, would not be required for the induction of cell elongation, which was first described using the G27 strain (48).

Next, we tested a variety of inhibitors of signaling pathways that lead to Arp2/3-dependent actin polymerization and showed that Rho GTPase pathways and the Arp2/3 complex itself are dispensable for the elongation phenotype. We recognize the possibility that redundancy of Rho GTPases or incomplete inhibition by the dominant negative constructs could explain the persistence of *H. pylori*-induced elongation in the treated cells. However, under conditions where our reagents inhibited other actin-based phenomena (*H. pylori* entry into AGS cells and *L. monocytogenes* intracellular movement), we observed no effect on *H. pylori*-induced cell elongation. Our finding that Arp2/3-depleted cells were still motile is consistent with a recent report that Arp2/3 activity is dispensable for cell motility in fibroblasts (14).

At first glance, our results appear to be in conflict with the finding that CagA-induced cell scattering is mediated by Rac1 signaling through WAVE (53). However, in their study Suzuki et al. directly measured only cell scattering, not elongation, although they used the two terms interchangeably. Here we

defined elongation as the hummingbird phenotype originally described by Segal et al. (48). Multiple reports attest to the fact that cellular elongation and cell scattering are two distinct phenotypes. Cell elongation is strictly dependent on CagA delivery and tyrosine phosphorylation (23, 39, 48; this study). Cell scattering appears to be an intrinsic property of AGS cells grown in serum (Fig. 6A and 7A); under some conditions it is enhanced by *H. pylori* infection but is only partially dependent on CagA activity (1, 39). Our method of measuring the elongation phenotype relies on the quantitative and unambiguous metrics of cell length and breadth, and it scores only the subset of cells that are transfected (8). In other studies workers used a qualitative rather than quantitative measure of cell shape, and in some cases, they did not distinguish between transfected cells expressing the protein of interest and nontransfected neighbors (1, 22–25, 39, 57).

Our finding that *H. pylori* induces elongation via a cell retraction defect is supported by the recent observations of Tsutsumi et al., who identified focal adhesion kinase (FAK) as a downstream target of CagA-activated SHP-2 (57). In the experiments of these workers, transfection of AGS cells with wild-type CagA caused a decrease in FAK tyrosine phosphorylation. Tsutsumi et al. proposed that a decrease in FAK activity led to an increase in focal adhesion turnover and thus greater cell motility, although they did not investigate cell movement in real time. Interestingly, they noted that although FAK activity decreased overall in cells expressing CagA, a pool of activated FAK in FA remained at the distal tips of cell extensions. FAK acts upon many substrates and can promote both FA assembly and disassembly (38, 42). FAK is also a direct target of the c-Met receptor tyrosine kinase and c-Src (10), both of which are key players in CagA signaling (7). Based on our finding that elongation is due to a cell retraction defect, we hypothesize that FAK stabilizes FA in the distal tips of elongating cells.

So far, the cell retraction defect induced by *H. pylori* CagA is unique among bacterial pathogens both in its Arp2/3-independent mechanism (18) and in its cellular phenomenology. However, the phenotype is reminiscent of the morphological change observed in epithelial cells following infection with vaccinia virus (46, 47). The vaccinia virus-induced phenotype is dependent upon suppression of RhoA signaling to Rho-associated kinase (ROCK) by the viral protein F11L (60). ROCK phosphorylates and activates myosin light chain of myosin II, an actin binding motor protein (33). Inhibition of ROCK with the chemical inhibitor Y-27632 leads to an elongated cell phenotype, likely through inhibition of myosin II phosphorylation (56). This has also been observed in myosin-null *Dictyostelium* that has a retraction defect during motility (58). We also found that direct inhibition of myosin II in AGS cells with blebbistatin, a specific inhibitor of the motor ATPase (51), results in an elongated cell phenotype reminiscent of *H. pylori* infection (unpublished observations). Furthermore, FAK is regulated by many of the same pathways that regulate myosin II activity. We attempted to use constitutively activated RhoA, constitutively active myosin light chain (56), and the catalytic domain of ameba PAK (54) to investigate the role of myosin II in CagA-induced AGS cell elongation. However, manipulation of these pathways appeared to cause a general loss of cellular adhesion, which confounded our L/B analysis (data not shown). Therefore, the role of myosin II in the CagA-induced retraction defect, if any, may be best explored in a different model system. Our studies with AGS cells have allowed us to rule out the hypothesis that the Cdc42/Rac1 and Arp2/3 pathways are pathways that contribute to the hummingbird phenotype. Our real-time imaging of *H. pylori*-infected cells demonstrated that the hummingbird phenotype is caused instead by a cell retraction defect and indicated that different molecular pathways are likely to be the target of CagA signaling in epithelial cells.

ACKNOWLEDGMENTS

We thank Ken Prehoda for technical assistance and Corrie Detweiler, Daniel Kalman, Barbara Kazmierczak, Daniel Portnoy, and Shiro Suetsugu for reagents. We also thank Andrei Ivanov, Clare Waterman-Storer, and the entire Guillemin lab for helpful discussions.

K.G. is a recipient of a Burroughs Wellcome Fund Career Award in the Biomedical Sciences and was supported by Research Scholar Grant RSG-03-101-01-MBC from the American Cancer Society and by NIH grant R56 DK075667-01.

REFERENCES

1. **Al-Ghoul, L., S. Wessler, T. Hundertmark, S. Kruger, W. Fischer, C. Wunder, R. Haas, A. Roessner, and M. Naumann.** 2004. Analysis of the type IV secretion system-dependent cell motility of Helicobacter pylori-infected epithelial cells. Biochem. Biophys. Res. Commun. **322:**860–866.
2. **Amieva, M. R., N. R. Salama, L. S. Tompkins, and S. Falkow.** 2002. Helicobacter pylori enter and survive within multivesicular vacuoles of epithelial cells. Cell. Microbiol. **4:**677–690.
3. **Backert, S., S. Moese, M. Selbach, V. Brinkmann, and T. F. Meyer.** 2001. Phosphorylation of tyrosine 972 of the Helicobacter pylori CagA protein is essential for induction of a scattering phenotype in gastric epithelial cells. Mol. Microbiol. **42:**631–644.
4. **Bagnoli, F., L. Buti, L. Tompkins, A. Covacci, and M. R. Amieva.** 2005. Helicobacter pylori CagA induces a transition from polarized to invasive phenotypes in MDCK cells. Proc. Natl. Acad. Sci. USA **102:**16339–16344.
5. **Benard, V., B. P. Bohl, and G. M. Bokoch.** 1999. Characterization of rac and cdc42 activation in chemoattractant-stimulated human neutrophils using a novel assay for active GTPases. J. Biol. Chem. **274:**13198–13204.
6. **Blaser, M. J., and J. C. Atherton.** 2004. Helicobacter pylori persistence: biology and disease. J. Clin. Investig. **113:**321–333.
7. **Bourzac, K. M., and K. Guillemin.** 2005. Helicobacter pylori-host cell interactions mediated by type IV secretion. Cell. Microbiol. **7:**911–919.
8. **Bourzac, K. M., L. A. Satkamp, and K. Guillemin.** 2006. The *Helicobacter pylori cag* pathogenicity island protein CagN is a bacterial membrane-associated protein that is processed at its C terminus. Infect. Immun. **74:**2537–2543.
9. **Chen, L. M., S. Hobbie, and J. E. Galan.** 1996. Requirement of CDC42 for Salmonella-induced cytoskeletal and nuclear responses. Science **274:**2115–2118.
10. **Chen, S. Y., and H. C. Chen.** 2006. Direct interaction of focal adhesion kinase (FAK) with Met is required for FAK to promote hepatocyte growth factor-induced cell invasion. Mol. Cell. Biol. **26:**5155–5167.
11. **Churin, Y., E. Kardalinou, T. F. Meyer, and M. Naumann.** 2001. Pathogenicity island-dependent activation of Rho GTPases Rac1 and Cdc42 in Helicobacter pylori infection. Mol. Microbiol. **40:**815–823.
12. **Covacci, A., S. Censini, M. Bugnoli, R. Petracca, D. Burroni, G. Macchia, A. Massone, E. Papini, Z. Xiang, N. Figura, et al.** 1993. Molecular characterization of the 128-kDa immunodominant antigen of Helicobacter pylori associated with cytotoxicity and duodenal ulcer. Proc. Natl. Acad. Sci. USA **90:**5791–5795.
13. **Criss, A. K., D. M. Ahlgren, T. S. Jou, B. A. McCormick, and J. E. Casanova.** 2001. The GTPase Rac1 selectively regulates Salmonella invasion at the apical plasma membrane of polarized epithelial cells. J. Cell Sci. **114:**1331–1341.
14. **Di Nardo, A., G. Cicchetti, H. Falet, J. H. Hartwig, T. P. Stossel, and D. J. Kwiatkowski.** 2005. Arp2/3 complex-deficient mouse fibroblasts are viable and have normal leading-edge actin structure and function. Proc. Natl. Acad. Sci. USA **102:**16263–16268.
15. **Ehrlich, J. S., M. D. Hansen, and W. J. Nelson.** 2002. Spatio-temporal regulation of Rac1 localization and lamellipodia dynamics during epithelial cell-cell adhesion. Dev. Cell **3:**259–270.
16. **Erickson, J. W., C. Zhang, R. A. Kahn, T. Evans, and R. A. Cerione.** 1996. Mammalian Cdc42 is a brefeldin A-sensitive component of the Golgi apparatus. J. Biol. Chem. **271:**26850–26854.
17. **Finlay, B. B.** 2005. Bacterial virulence strategies that utilize Rho GTPases. Curr. Top. Microbiol. Immunol. **291:**1–10.

18. **Gouin, E., M. D. Welch, and P. Cossart.** 2005. Actin-based motility of intracellular pathogens. Curr. Opin. Microbiol. **8:**35–45.
19. **Guillemin, K., N. R. Salama, L. S. Tompkins, and S. Falkow.** 2002. Cag pathogenicity island-specific responses of gastric epithelial cells to Helicobacter pylori infection. Proc. Natl. Acad. Sci. USA **99:**15136–15141.
20. **Harlander, R. S., M. Way, Q. Ren, D. Howe, S. S. Grieshaber, and R. A. Heinzen.** 2003. Effects of ectopically expressed neuronal Wiskott-Aldrich syndrome protein domains on *Rickettsia rickettsii* actin-based motility. Infect. Immun. **71:**1551–1556.
21. **Hatakeyama, M.** 2003. Helicobacter pylori CagA—a potential bacterial oncoprotein that functionally mimics the mammalian Gab family of adaptor proteins. Microbes Infect. **5:**143–150.
22. **Higashi, H., A. Nakaya, R. Tsutsumi, K. Yokoyama, Y. Fujii, S. Ishikawa, M. Higuchi, A. Takahashi, Y. Kurashima, Y. Teishikata, S. Tanaka, T. Azuma, and M. Hatakeyama.** 2004. Helicobacter pylori CagA induces Ras-independent morphogenetic response through SHP-2 recruitment and activation. J. Biol. Chem. **279:**17205–17216.
23. **Higashi, H., R. Tsutsumi, A. Fujita, S. Yamazaki, M. Asaka, T. Azuma, and M. Hatakeyama.** 2002. Biological activity of the Helicobacter pylori virulence factor CagA is determined by variation in the tyrosine phosphorylation sites. Proc. Natl. Acad. Sci. USA **99:**14428–14433.
24. **Higashi, H., R. Tsutsumi, S. Muto, T. Sugiyama, T. Azuma, M. Asaka, and M. Hatakeyama.** 2002. SHP-2 tyrosine phosphatase as an intracellular target of Helicobacter pylori CagA protein. Science **295:**683–686.
25. **Higuchi, M., R. Tsutsumi, H. Higashi, and M. Hatakeyama.** 2004. Conditional gene silencing utilizing the lac repressor reveals a role of SHP-2 in cagA-positive Helicobacter pylori pathogenicity. Cancer Sci. **95:**442–447.
26. **Hirsch, D. S., D. M. Pirone, and P. D. Burbelo.** 2001. A new family of Cdc42 effector proteins, CEPs, function in fibroblast and epithelial cell shape changes. J. Biol. Chem. **276:**875–883.
27. **Itoh, R. E., K. Kurokawa, Y. Ohba, H. Yoshizaki, N. Mochizuki, and M. Matsuda.** 2002. Activation of rac and cdc42 video imaged by fluorescent resonance energy transfer-based single-molecule probes in the membrane of living cells. Mol. Cell. Biol. **22:**6582–6591.
28. **Johnson, D. I.** 1999. Cdc42: An essential Rho-type GTPase controlling eukaryotic cell polarity. Microbiol. Mol. Biol. Rev. **63:**54–105.
29. **Kraynov, V. S., C. Chamberlain, G. M. Bokoch, M. A. Schwartz, S. Slabaugh, and K. M. Hahn.** 2000. Localized Rac activation dynamics visualized in living cells. Science **290:**333–337.
30. **Kwok, T., S. Backert, H. Schwarz, J. Berger, and T. F. Meyer.** 2002. Specific entry of *Helicobacter pylori* into cultured gastric epithelial cells via a zipper-like mechanism. Infect. Immun. **70:**2108–2120.
31. **Machesky, L. M., and R. H. Insall.** 1998. Scar1 and the related Wiskott-Aldrich syndrome protein, WASP, regulate the actin cytoskeleton through the Arp2/3 complex. Curr. Biol. **8:**1347–1356.
32. **Machesky, L. M., R. D. Mullins, H. N. Higgs, D. A. Kaiser, L. Blanchoin, R. C. May, M. E. Hall, and T. D. Pollard.** 1999. Scar, a WASp-related protein, activates nucleation of actin filaments by the Arp2/3 complex. Proc. Natl. Acad. Sci. USA **96:**3739–3744.
33. **Matsumura, F.** 2005. Regulation of myosin II during cytokinesis in higher eukaryotes. Trends Cell Biol. **15:**371–377.
34. **May, R. C., M. E. Hall, H. N. Higgs, T. D. Pollard, T. Chakraborty, J. Wehland, L. M. Machesky, and A. S. Sechi.** 1999. The Arp2/3 complex is essential for the actin-based motility of Listeria monocytogenes. Curr. Biol. **9:**759–762.
35. **Michaelson, D., J. Silletti, G. Murphy, P. D'Eustachio, M. Rush, and M. R. Philips.** 2001. Differential localization of Rho GTPases in live cells: regulation by hypervariable regions and RhoGDI binding. J. Cell Biol. **152:**111–126.
36. **Miki, H., S. Suetsugu, and T. Takenawa.** 1998. WAVE, a novel WASP-family protein involved in actin reorganization induced by Rac. EMBO J. **17:**6932–6941.
37. **Miki, H., and T. Takenawa.** 2003. Regulation of actin dynamics by WASP family proteins. J. Biochem. (Tokyo) **134:**309–313.
38. **Mitra, S. K., D. A. Hanson, and D. D. Schlaepfer.** 2005. Focal adhesion kinase: in command and control of cell motility. Nat. Rev. Mol. Cell. Biol. **6:**56–68.
39. **Moese, S., M. Selbach, T. Kwok, V. Brinkmann, W. Konig, T. F. Meyer, and S. Backert.** 2004. *Helicobacter pylori* induces AGS cell motility and elongation via independent signaling pathways. Infect. Immun. **72:**3646–3649.
40. **Moreau, V., F. Frischknecht, I. Reckmann, R. Vincentelli, G. Rabut, D. Stewart, and M. Way.** 2000. A complex of N-WASP and WIP integrates signalling cascades that lead to actin polymerization. Nat. Cell Biol. **2:**441–448.
41. **Oh, J. D., S. M. Karam, and J. I. Gordon.** 2005. Intracellular Helicobacter pylori in gastric epithelial progenitors. Proc. Natl. Acad. Sci. USA **102:**5186–5191.
42. **Parsons, J. T.** 2003. Focal adhesion kinase: the first ten years. J. Cell Sci. **116:**1409–1416.
43. **Pertz, O., and K. M. Hahn.** 2004. Designing biosensors for Rho family proteins—deciphering the dynamics of Rho family GTPase activation in living cells. J. Cell Sci. **117:**1313–1318.
44. **Raftopoulou, M., and A. Hall.** 2004. Cell migration: Rho GTPases lead the way. Dev. Biol. **265:**23–32.
45. **Ridley, A. J., M. A. Schwartz, K. Burridge, R. A. Firtel, M. H. Ginsberg, G. Borisy, J. T. Parsons, and A. R. Horwitz.** 2003. Cell migration: integrating signals from front to back. Science **302:**1704–1709.
46. **Sanderson, C. M., and G. L. Smith.** 1998. Vaccinia virus induces Ca^{2+}-independent cell matrix adhesion during the motile phase of infection. J. Virol. **72:**9924–9933.
47. **Sanderson, C. M., M. Way, and G. L. Smith.** 1998. Virus-induced cell motility. J. Virol. **72:**1235–1243.
48. **Segal, E. D., J. Cha, J. Lo, S. Falkow, and L. S. Tompkins.** 1999. Altered states: involvement of phosphorylated CagA in the induction of host cellular growth changes by Helicobacter pylori. Proc. Natl. Acad. Sci. USA **96:**14559–14564.
49. **Selbach, M., S. Moese, C. R. Hauck, T. F. Meyer, and S. Backert.** 2002. Src is the kinase of the Helicobacter pylori CagA protein in vitro and in vivo. J. Biol. Chem. **277:**6775–6778.
50. **Stein, M., F. Bagnoli, R. Halenbeck, R. Rappuoli, W. J. Fantl, and A. Covacci.** 2002. c-Src/Lyn kinases activate Helicobacter pylori CagA through tyrosine phosphorylation of the EPIYA motifs. Mol. Microbiol. **43:**971–980.
51. **Straight, A. F., A. Cheung, J. Limouze, I. Chen, N. J. Westwood, J. R. Sellers, and T. J. Mitchison.** 2003. Dissecting temporal and spatial control of cytokinesis with a myosin II Inhibitor. Science **299:**1743–1747.
52. **Suetsugu, S., H. Miki, and T. Takenawa.** 1999. Identification of two human WAVE/SCAR homologues as general actin regulatory molecules which associate with the Arp2/3 complex. Biochem. Biophys. Res. Commun. **260:**296–302.
53. **Suzuki, M., H. Mimuro, T. Suzuki, M. Park, T. Yamamoto, and C. Sasakawa.** 2005. Interaction of CagA with Crk plays an important role in Helicobacter pylori-induced loss of gastric epithelial cell adhesion. J. Exp. Med. **202:**1235–1247.
54. **Szczepanowska, J., E. D. Korn, and H. Brzeska.** 2006. Activation of myosin in HeLa cells causes redistribution of focal adhesions and F-actin from cell center to cell periphery. Cell Motil. Cytoskeleton **63:**356–374.
55. **Tafazoli, F., K. E. Magnusson, and L. Zheng.** 2003. Disruption of epithelial barrier integrity by *Salmonella enterica* serovar Typhimurium requires geranylgeranylated proteins. Infect. Immun. **71:**872–881.
56. **Totsukawa, G., Y. Wu, Y. Sasaki, D. J. Hartshorne, Y. Yamakita, S. Yamashiro, and F. Matsumura.** 2004. Distinct roles of MLCK and ROCK in the regulation of membrane protrusions and focal adhesion dynamics during cell migration of fibroblasts. J. Cell Biol. **164:**427–439.
57. **Tsutsumi, R., A. Takahashi, T. Azuma, H. Higashi, and M. Hatakeyama.** 2006. Focal adhesion kinase is a substrate and downstream effector of SHP-2 complexed with Helicobacter pylori CagA. Mol. Cell. Biol. **26:**261–276.
58. **Uchida, K. S., T. Kitanishi-Yumura, and S. Yumura.** 2003. Myosin II contributes to the posterior contraction and the anterior extension during the retraction phase in migrating Dictyostelium cells. J. Cell Sci. **116:**51–60.
59. **Unsworth, K. E., M. Way, M. McNiven, L. Machesky, and D. W. Holden.** 2004. Analysis of the mechanisms of Salmonella-induced actin assembly during invasion of host cells and intracellular replication. Cell. Microbiol. **6:**1041–1055.
60. **Valderrama, F., J. V. Cordeiro, S. Schleich, F. Frischknecht, and M. Way.** 2006. Vaccinia virus-induced cell motility requires F11L-mediated inhibition of RhoA signaling. Science **311:**377–381.
61. **Vazquez-Torres, A., J. Jones-Carson, A. J. Baumler, S. Falkow, R. Valdivia, W. Brown, M. Le, R. Berggren, W. T. Parks, and F. C. Fang.** 1999. Extraintestinal dissemination of Salmonella by CD18-expressing phagocytes. Nature **401:**804–808.
62. **Vogt, A., Y. Qian, T. F. McGuire, A. D. Hamilton, and S. M. Sebti.** 1996. Protein geranylgeranylation, not farnesylation, is required for the G1 to S phase transition in mouse fibroblasts. Oncogene **13:**1991–1999.
63. **Welch, M. D., A. Iwamatsu, and T. J. Mitchison.** 1997. Actin polymerization is induced by Arp2/3 protein complex at the surface of Listeria monocytogenes. Nature **385:**265–269.
64. **Welch, M. D., and R. D. Mullins.** 2002. Cellular control of actin nucleation. Annu. Rev. Cell Dev. Biol. **18:**247–288.
65. **Wennerberg, K., and C. J. Der.** 2004. Rho-family GTPases: it's not only Rac and Rho (and I like it). J. Cell Sci. **117:**1301–1312.
66. **Wittmann, T., and C. M. Waterman-Storer.** 2001. Cell motility: can Rho GTPases and microtubules point the way? J. Cell Sci. **114:**3795–3803.

Editor: D. L. Burns